

SECURITY CLASS:

AD-A203 561

DOCUMENTATION PAGE

1a. REPORT SEC
Unclassif:

1b. RESTRICTIVE MARKINGS

DTIC FILE COPY

2a. SECURITY CL

3. DISTRIBUTION/AVAILABILITY OF REPORT
Approved for public release;
Distribution Unlimited

2b. DECLASSIFICATION/DOWNGRADING SCHEDULE

4. PERFORMING ORGANIZATION REPORT NUMBER(S)

5. MONITORING ORGANIZATION REPORT NUMBER(S)

AFGL-TR-89-0001

6a. NAME OF PERFORMING ORGANIZATION

6b. OFFICE SYMBOL
(if applicable)
LID

7a. NAME OF MONITORING ORGANIZATION

Air Force Geophysics Laboratory

7b. ADDRESS (City, State, and ZIP Code)

6c. ADDRESS (City, State, and ZIP Code)

Hanscom AFB
Massachusetts 01731-5000

8a. NAME OF FUNDING/SPONSORING ORGANIZATION

8b. OFFICE SYMBOL
(if applicable)

9. PROCUREMENT INSTRUMENT IDENTIFICATION NUMBER

8c. ADDRESS (City, State, and ZIP Code)

10. SOURCE OF FUNDING NUMBERS

PROGRAM ELEMENT NO.	PROJECT NO.	TASK NO.	WORK UNIT ACCESSION NO.
62101F	4643	14	02

11. TITLE (Include Security Classification)

Density Measurements With Combined Raman-Rayleigh Lidar

12. PERSONAL AUTHOR(S)

Phan Dao, Wayne Klemetti, Dwight Sipler; W.P. Moskowitz*; G. Davidson*

13a. TYPE OF REPORT
REPRINT

13b. TIME COVERED

FROM _____ TO _____

14. DATE OF REPORT (Year, Month, Day)

1989 January 3

15. PAGE COUNT

5

16. SUPPLEMENTARY NOTATION * Photometrics Inc, Woburn, MA 01801

Presented at SPIE's Symposium on Innovative Science & Technology for Govt and Civilian Applications, 15-20 January 1989, Los Angeles, CA

17. COSATI CODES

FIELD	GROUP	SUB-GROUP

18. SUBJECT TERMS (Continue on reverse if necessary and identify by block number)

Lidar Scattering
Rayleigh Neutral density
Raman Klett inversion

19. ABSTRACT (Continue on reverse if necessary and identify by block number)

A combined Raman-Rayleigh Lidar (Light Detection and Ranging) has recently been implemented at the Air Force Geophysics Laboratory's ground-based lidar station to measure neutral density from the lower stratosphere to the upper mesosphere. Rayleigh Lidar reliably measures relative densities in the region above 30 km. In this region, atmospheric extinction can be neglected and backscattering is primarily due to Rayleigh scattering. However, when density measurements are needed for the lower stratosphere two complications arise: the contribution of aerosol (Mie and Rayleigh) scattering to the Rayleigh signal and the effect of aerosol attenuation. Vibrational Raman scattering, being an elastic process for molecules only; can be used to resolve the first ambiguity. The second difficulty requires an inversion technique to help determine the attenuation profile from the Lidar signal and provide a transmission correction of this signal. For the lower stratosphere, the technique adopted in this laboratory is a three-step treatment of data. In step (1) Klett¹ inversion is applied on the elastic scattering signal (Mie and Rayleigh) to obtain a transmission altitude profile. In step (2) the molecular signal

20. DISTRIBUTION/AVAILABILITY OF ABSTRACT

UNCLASSIFIED/UNLIMITED SAME AS RPT. DTIC USERS

21. ABSTRACT SECURITY CLASSIFICATION

Unclassified

22a. NAME OF RESPONSIBLE INDIVIDUAL

Phan D. Dao

22b. TELEPHONE (Include Area Code)

(617) 377-4944

22c. OFFICE SYMBOL

AFGL/LID

2

CONT OF BLOCK 19:

from the Raman Lidar is corrected for atmospheric attenuation. In step (3), Raman data for below 25 km is spliced to Rayleigh data for above 25 km to give the entire profile of neutral density. Application of this analysis to experimental data will be shown and discussed.

Accession For	
NTIS GRA&I	<input checked="" type="checkbox"/>
DTIC TAB	<input checked="" type="checkbox"/>
Unannounced	<input type="checkbox"/>
Justification	
By _____	
Distribution/	
Availability Codes	
Dist	Avail and/or Special
A-1	



- 7 -

AFGL-TR-89-0001

Density measurements with combined Raman-Rayleigh LidarPhan Dao, Wayne Klemetti, and Dwight Sipler*
Air Force Geophysics Laboratory/LID, Hanscom AFB, Mass. 01731W.P. Moskowitz and G. Davidson
Photometrics, Inc., Woburn, Mass. 01801**ABSTRACT**

A combined Raman-Rayleigh Lidar (Light Detection And Ranging) has recently been implemented at the Air Force Geophysics Laboratory's ground-based lidar station to measure neutral density from the lower stratosphere to the upper mesosphere.

Rayleigh Lidar reliably measures relative densities in the region above 30 km. In this region, atmospheric extinction can be neglected and backscattering is primarily due to Rayleigh scattering. However, when density measurements are needed for the lower stratosphere two complications arise: the contribution of aerosol (Mie and Rayleigh) scattering to the Rayleigh signal and the effect of aerosol attenuation. Vibrational Raman scattering, being an elastic process for molecules only, can be used to resolve the first ambiguity. The second difficulty requires an inversion technique to help determine the attenuation profile from the Lidar signal and provide a transmission correction of this signal.

For the lower stratosphere, the technique adopted in this laboratory is a three-step treatment of data. In step (1) Klett inversion is applied on the elastic scattering signal (Mie and Rayleigh) to obtain a transmission altitude profile. In step (2) the molecular signal from the Raman Lidar is corrected for atmospheric attenuation. In step (3), Raman data for below 25 km is spliced to Rayleigh data for above 25 km to give the entire profile of neutral density. Application of this analysis to experimental data will be shown and discussed.

1. INTRODUCTION

Under normal conditions elastically backscattered light from the 30-90 km range corresponds to that expected from Rayleigh scattering by atmospheric molecules². With commercially available high-power lasers and improved electronic detection systems, Rayleigh Lidar has become a reliable tool in determining neutral density in the middle atmosphere. Furthermore, with increased laser power and stronger signal strength, measurements for small intervals of signal integration are possible. This opens up the possibility of studying short time-scale density perturbations such as those caused by acoustic gravity waves³.

Lidar measurements are also difficult to calibrate as signal strength depends on transmitting and receiving efficiencies. These vary with meteorological conditions as well as instrumental conditions. Fortunately, instrumental changes can be quantified and the atmosphere does not change during the beam round trip time. These imply that after proper corrections for atmospheric transmission, Lidar signals can be reduced to a relative neutral density profile. Therefore only one calibration point is required for the entire density profile. Slow changes of the atmosphere require independent measurements for calibration. Rawinsonde balloons can be released so that they floating above the Lidar site when attaining the altitude of calibration.

Raman Lidar has been implemented to measure density profile for various molecular components

* current affiliation: M. I. T. Haystack Observatory, Westford, Massachusetts.

X- 89 1 09 225

of the atmosphere⁴. Since Raman signal is spectrally separate from Rayleigh and Mie signals, it depends only on the density of the molecule of interest⁵. Together with the Klett technique, this utility helps obtain transmission-corrected absolute neutral densities in the regions below and above the rawinsonde calibration point. We will discuss (a) the Laboratory Lidar and its operations, (b) the Raman augmentation and (c) Rayleigh-Raman combined absolute density measurements.

2. AFGL LABORATORY LIDAR

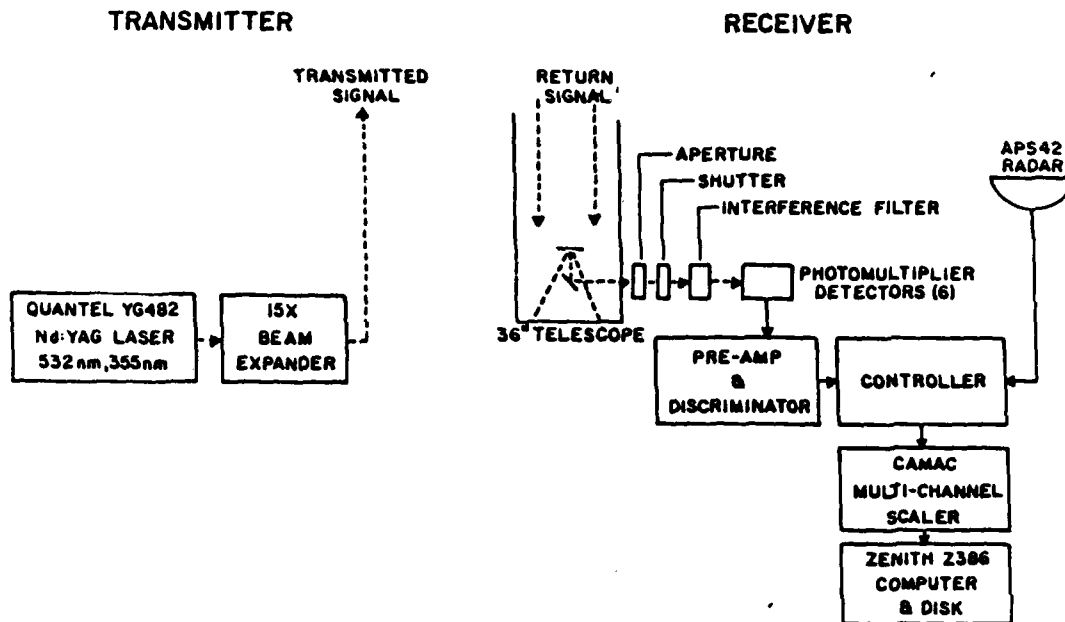


Figure 1 LIDAR Block Diagram

AFGL has two Lidar systems: a laboratory system (GLEAM, Ground-based Lidar Experiments of Atmospheric Measurements) and a mobile version for field measurements (GLINT, Ground-based Lidar Investigation-Transportable). The Raman capability has been implemented in the GLEAM system which consists of a Nd:YAG laser transmitter and a f/15 36 inch Dall-Kirkham telescope. The frequency-doubled and -tripled outputs of the Nd:YAG, at 532 and 355 nm respectively, is beam-expanded with a magnification of 15x and transmitted vertically. The transmitted laser beam has a divergence of 0.05 mrad which is small compared to the telescope field of view. The laser is operated at a repetition rate of 10 Hz and pulse energies are maintained at ca. 250 mJ for green and 60 mJ for UV output. Scattered radiation is collected with a telescope field of view which is ca. 1.5 mrad. The returned light is mechanically shuttered, split, attenuated and coupled to a 6 photomultiplier (PMT) detection system. The latter consists of a green and a UV channel, each channel having a high, a medium and a low altitude PMT. The use of beam splitters and attenuators ensures that the Lidar returns falls in the optimum dynamic range of each PMT. For most applications, the return is photon counted. Photons are counted with Camac-based multichannel scalers and recorded with a personal computer. A safety radar is used for aircraft avoidance. Fig. 1 shows the Lidar block diagram. For this study, the scaler dwell time is set at 2 μ s and represents a range resolution of 0.3 km.

A 12 inch telescope collects the Raman signal. An interference filter of 10 nm bandpass centered at 386 nm is used to spectrally select the first Stokes scattered radiation from nitrogen molecules. The Raman signal is photon-counted and integrated with a multichannel scaler. Since the Raman signal is 4 orders of magnitude smaller than the Rayleigh signal, 3 orders for the difference in scattering cross

sections and 1 order for the difference in telescope apertures, only one photomultiplier is used for the Raman return. The Rayleigh signals from the 36-inch telescope and Raman from the 12-inch telescope are collected simultaneously. In the basic data files, these signals are integrated over 5 minutes or 3000 laser pulses. Laser energies are also recorded for post-experiment power correction.

Rawinsonde balloons released at 0000Z in Albany, New York (130 miles, West), Portland, Maine (95 miles, North East), and Chatham, Massachusetts (85 miles, South East) provide density measurements from ground level to about 25-30 km. The density profiles obtained with the slowly ascending balloon are path-dependent and cannot be directly compared with the real-time measurements of Lidar. The calibration procedure ties the Lidar density to a Rawinsonde data point at 25 km.

3. TRANSMISSION CORRECTION WITH KLETT INVERSION:

To correct for attenuation in the region below 30 km, it is necessary to consider atmospheric attenuation and aerosol (Mie and Rayleigh) scattering. The combined Raman-Rayleigh Lidar solves both problems with the following technique. We have transmitted radiation at two wavelengths: 532 and 355 nm. The green signal is received at the unshifted wavelength for Rayleigh data. The UV signal is received at unshifted and at Stokes-shifted wavelengths -355 and 386 nm for nitrogen molecules, respectively. The Rayleigh signal is free of aerosol scattering for the region above 25 km. Aerosol anomalies higher than 25 km such as noctilucent clouds would be detected in the green/UV ratio profile. The Raman signal is free of aerosol scattering but nevertheless attenuated in the round-trip through the lower atmosphere. The transmission at 355 nm is determined by the inversion of the Rayleigh signal at 355 nm. Note that the round-trip attenuation of the Raman signal is for 355 nm wavelength on the way up and 386 nm on the way down but the difference due to the wavelength shift is neglected on valid grounds. Above 25 km, the integrated transmission is expected to level off and for that reason, the 532 nm Rayleigh signal is used in density analysis without correction for transmission. The transmission-corrected density profile (at low altitudes) produced by Raman Lidar is spliced to the 532 nm Rayleigh profile (at high altitudes) to form a single profile from 10 to 80 km. Figure 2 shows the road map of data analysis.

The Klett technique is based on the assumption that the backscattering coefficient can be expressed as a function of the extinction coefficient in an equation, usually referred to as the power law:

$$\beta = \text{const } \sigma^k \quad (1)$$

where k is a constant reported to be smaller than 1 and greater than 0.67⁶. The atmospheric conditions of greatest interest to Lidar experiments are those where molecular scattering is stronger than aerosol scattering in the region where density is to be determined. Haze and optically thin cloud in the boundary layer does not affect the inversion since Klett algorithm is worked downward and stopped at a height of 10 km. Under the mentioned conditions, k is expected to be close to 1 in the region of interest. Klett showed that the extinction coefficient along the line-of-sight depends on the signal strength as described by

$$\sigma(r) = \frac{\exp\left[\frac{S-S_M}{k}\right]}{\sigma_M + \frac{2}{k} \int_r^{r_M} \exp\left[\frac{S(x)-S_M}{k}\right] dx} \quad (2)$$

In the expression, $S(r)$ is the range corrected logarithmic photon count at range r and defined as

$$S(r) = \ln(r^2 \cdot N(r)) \quad (3)$$

where $N(r)$ is the photon count (signal) at range r . The use of (2) requires the knowledge of the extinction coefficient σ_M at range r_M , typically between 25 and 30 km. In this region molecular scattering is



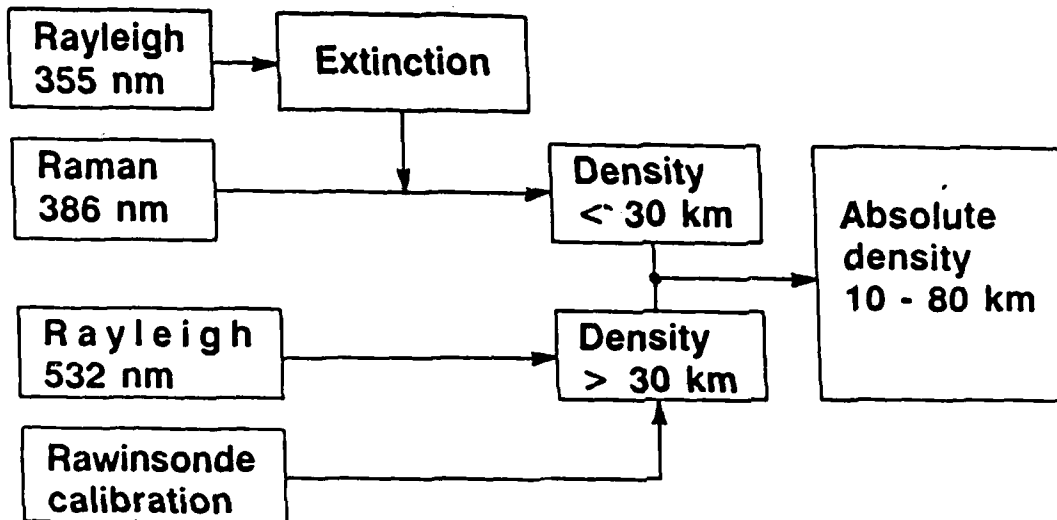


Figure 2 Data Block Diagram

predominant, density is known from Rawinsonde measurement and the extinction coefficient is readily approximated.

Figure 3 shows a typical 355 nm Lidar unprocessed data. Laser energy is 150 mJ/pulse and laser repetition rate is 10 Hz. Signal is received with the 36 inch dia telescope and integrated for 30 minutes. The signal from below 8 km is modulated by the opening of the mechanical shutter and the overlap of the telescope field-of-view and the beam. The shutter is fully open and the overlap is total above 8 km. Figure 4 shows the corresponding Klett-inverted integrated transmission profile at low altitudes. The values shown correspond to round trip transmission between 9.7 km and the point of interest. In the inversion, we have use 0.00027 /km as the extinction coefficient at 30 km⁷. The inversion result has been shown not to depend critically on this estimate¹. The curve in Figure 4 indicates that density would be overestimated by 20% at 10 km were atmospheric extinction not accounted for and the calibration tie made at 30 km. The curves also indicates that the integrated transmission has levelled off by and above 25 km. This allows the use of uncorrected Rayleigh signal above 25 km.

4. COMBINED DENSITY PROFILES

Figure 5 shows the combined neutral density ratio to the USSA76 standard. The profile is measured at Hanscom Air Force Base, on September 19, 1988 at 0200-0230Z. The transmission-corrected Raman density profile for the 10-25 km range (lower) is spliced to the Rayleigh 10-70 km density profile (upper). Both curves have a 1.5 km vertical resolution and a 30 minute integration time. The Rayleigh profile for the 10-25 km range is shown to demonstrate the effect of atmospheric extinction. The valid density profile is composed of the Raman profile below 25 km and the Rayleigh profile above 25 km.

In this laboratory (result shown in Fig. 5), Raman signal is obtained with the 355 nm beam and

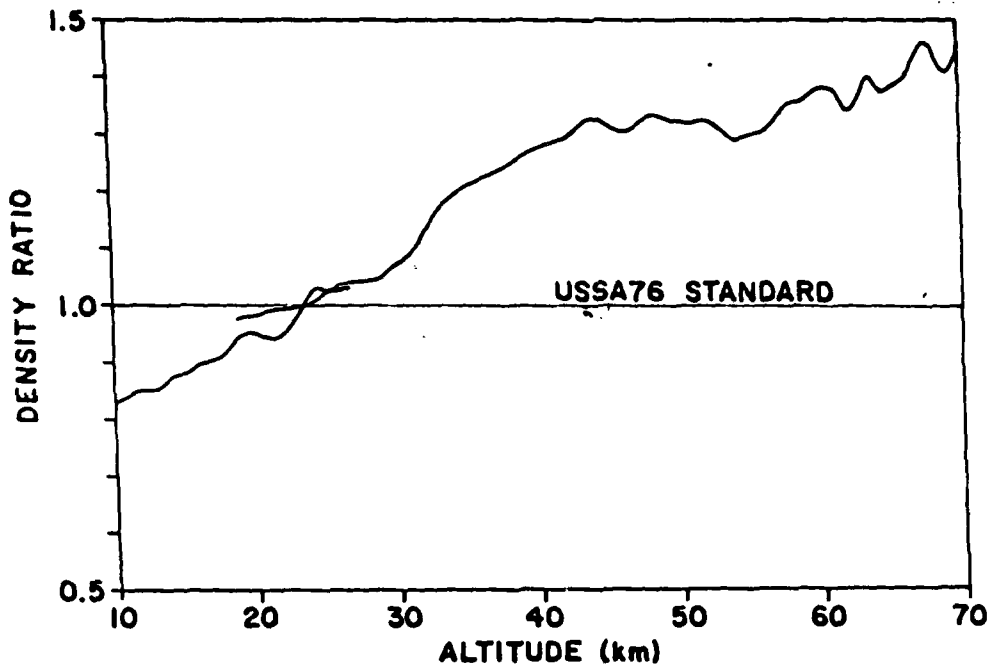


Figure 5 Combined Raman-Rayleigh density profile. Raman profile (lower trace and extending from 10 to 25 km) has been corrected for transmission. Rayleigh profile (upper trace and from 10 to 70 km) is also shown.

1. J. Klett, *Applied Optics*, 20, 211 (1981).
2. G. S. Kent and R. W. H. Wright, *Atmospheric and Terrestrial Physics*, 33, 917 (1970).
3. C. R. Philbrick, D. P. Sipler, G. Davidson and W. P. Moskowitz, *Optical Society Topical Meeting on Laser and Optical Remote Sensing: Instrumentation and Techniques*, 18, North Falmouth, Mass., Sept. 28 - Oct. 1, 1987.
4. H. Inaba and T. Kobayasi, *Nature*, 224, 170 (1969).
5. W. P. Moskowitz, G. Davidson, D. Sipler, C. R. Philbrick and P. Dao, *International Laser Radar Conference*, 14, Innichen-San Candido, Italy, June 20-24, 1988.
6. J. A. Curcio and G. L. Knestruck, *J. Opt. Soc. Am.*, 48, 686 (1958); R. W. Fenn, *Appl. Opt.*, 5, 293 (1966); S. Twomey and H. B. Howell, *Appl. Opt.*, 4, 501 (1965).
7. R. A. McClatchey, R. W. Fenn, J. E. A. Selby, F. E. Volz and J. S. Garing, *Handbook of Optics*, ed. W. G. Driscoll and W. Vaughan, Optical Society of America, 14-1 (1978).